

Supplementary Information for

Hydrocracking of Polyolefins over Ceria-promoted Ni/BEA Catalysts

Jessie A. Sun^{1,2}, Esun Selvam^{1,2}, Alexander Bregvadze¹, Weiqing Zheng¹, Dionisios G. Vlachos^{1,2,3*}

¹Department of Chemical and Biomolecular Engineering, University of Delaware, 150 Academy St., Newark, DE 19716, USA

²Center for Plastics Innovation, University of Delaware, 221 Academy St., Newark, DE 19716, USA

³Delaware Energy Institute, University of Delaware, 221 Academy St., Newark, DE, 19716, USA

*Corresponding author. Email: vlachos@udel.edu

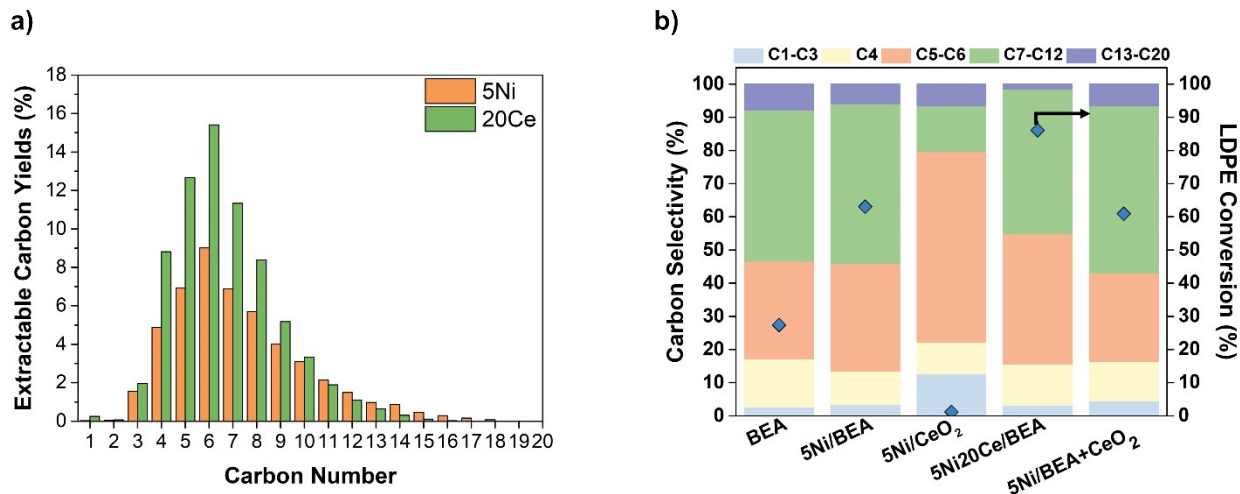


Figure S1. **a)** Carbon product distribution for LDPE hydrocracking over 5Ni/BEA (5Ni) and 5Ni20Ce/BEA (20Ce) catalyst. Reaction conditions: 1 h reaction at 300 °C, 30 bar H₂, 2 g LDPE, 0.025 g catalyst. **b)** LDPE hydrocracking product selectivity distributions for physical mixture experiments (activity trends shown in Figure 1d). Catalyst mixtures with the same metal wt.% (5% Ni and 20% Ce) were maintained within the mixture experiments.

Table S1. Reaction conditions used for naphtha productivity comparison (Figure 1c) of reported hydrocracking catalysts from literature.

Catalyst	Naphtha Productivity ($\text{g}_{\text{naphtha}}^* / \text{g}_{\text{cat}}^{-1} \cdot \text{h}^{-1}$)	Naphtha Yield (%)	Catalyst (g)	Initial Polymer (g)	Time (h)	Temp (°C)	Pressure (bar)	Polymer	Lit. Ref #
Ni/BEA	15	15	0.02	2	1	250	60	LDPE	20
Pt/BEA	9	18	0.02	2	2	250	60	LDPE	20
Ce-PtSn/SiAl	38.5	77	0.02	2	2	270	30	HDPE	13
PtSn/SiAl	25	50	0.02	2	2	270	30	HDPE	13
Pt/WO ₃ /ZrO ₂ + BEA	2.85	57	0.2	2	2	250	30	LDPE	15
Ru/BEA	0.45	51	0.05	0.7	16	200	30	LDPE	12
Pt@S-1	4.45	89	0.2	2	2	250	30	LDPE	16
Ce-Pt/HY	4.25	85	0.2	2	2	280	20	LDPE	14
Ni/ZSM-5	0.19	37.5	0.2	1.59	16	375	45	LDPE	11
Co/ZSM-5	0.20	40.3	0.2	1.59	16	375	45	LDPE	11
Ni-WO _x ZrO ₂	3.07	64	0.25	2	100 ^a	260	30	LDPE	18

^a - Reaction time in minutes

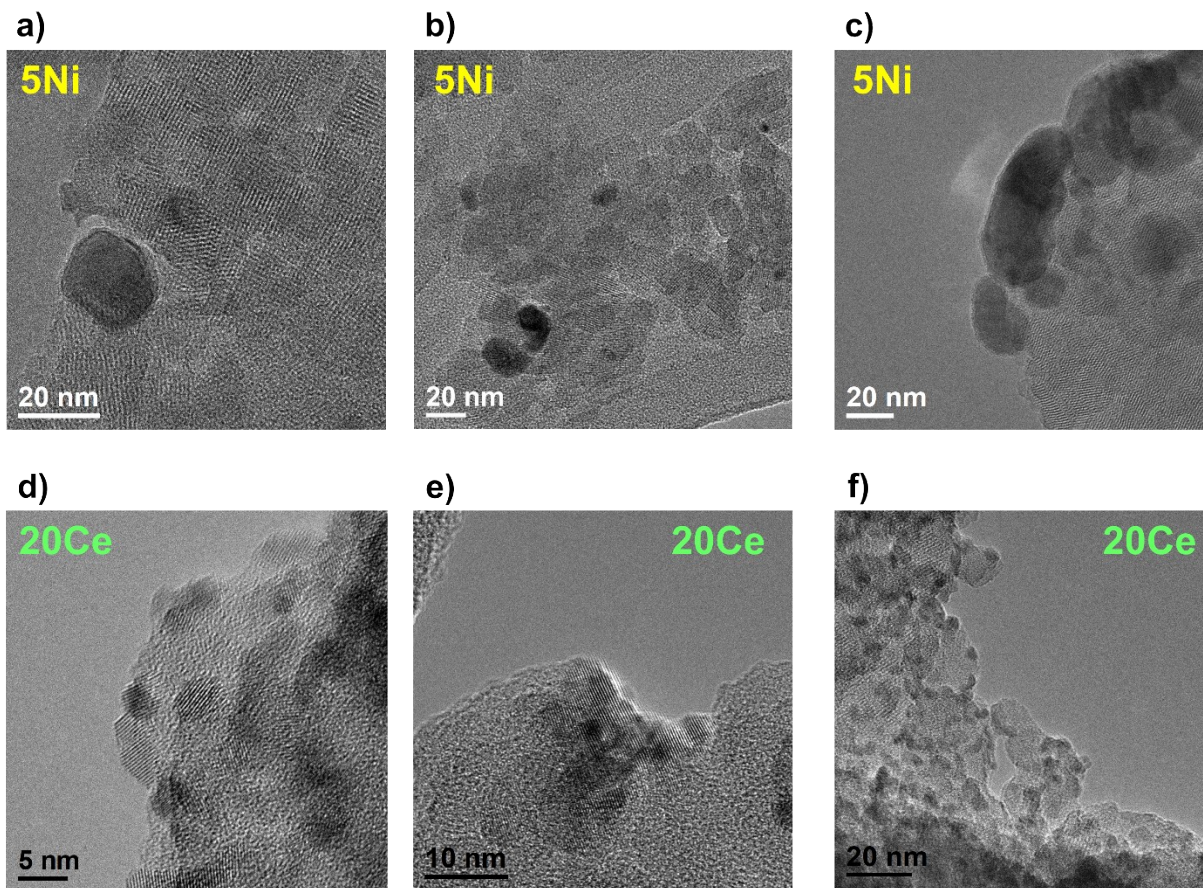


Figure S2. a-c) HRTEM micrographs depicting agglomeration of large nanoparticles from sintering in 5Ni/BEA (5Ni) catalyst. d) Images of 5Ni20Ce/BEA (20Ce) catalyst depicting some isolated Ni nanoparticles on BEA support and e) Ni nanoparticles near CeO₂ nanoparticles in proximity. f) 20Ce catalyst with smaller nanoparticles without the formation of large aggregates.

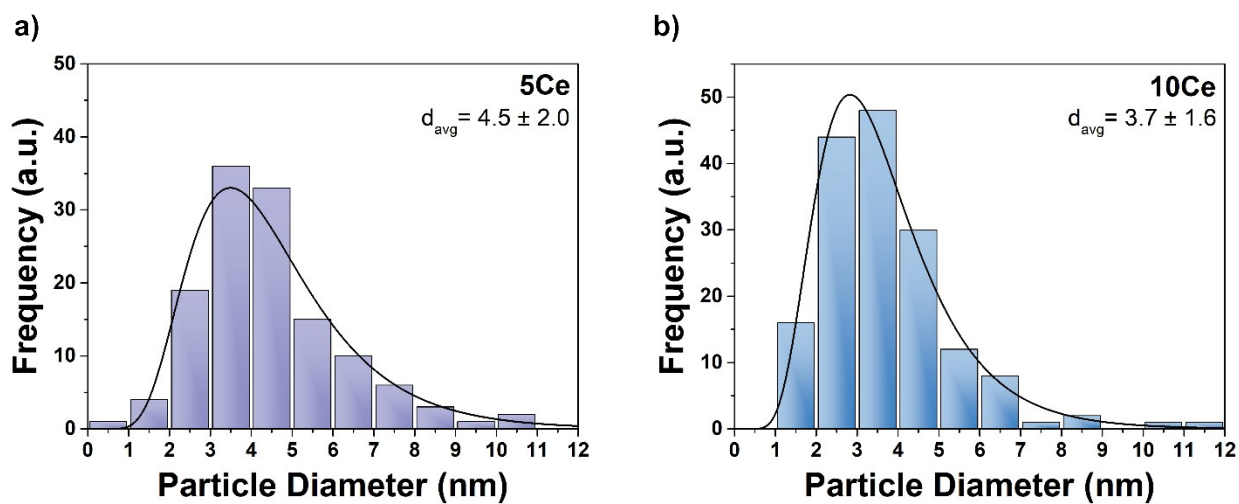


Figure S3. Lognormal particle size distributions from HRTEM measurements for a) 5Ni5Ce/BEA (5Ni) – [131 particle count] and b) 5Ni10Ce/BEA (10Ce) – [163 particle count].

Table S2. X-ray fluorescent spectroscopy (XRF) was performed to verify elemental Ni% and Ce% composition in Ce-promoted 5Ni/BEA catalysts (%Ce = 0, 5, 10, 20).

Catalyst	Theoretical % Ni	XRF %Ni	Theoretical %Ce	XRF %Ce
5Ni	5	4.7	0	0
5Ni5Ce	5	5.5	5	7.6
5Ni10Ce	5	5.7	10	12.0
5Ni20Ce	5	5.1	20	23.6

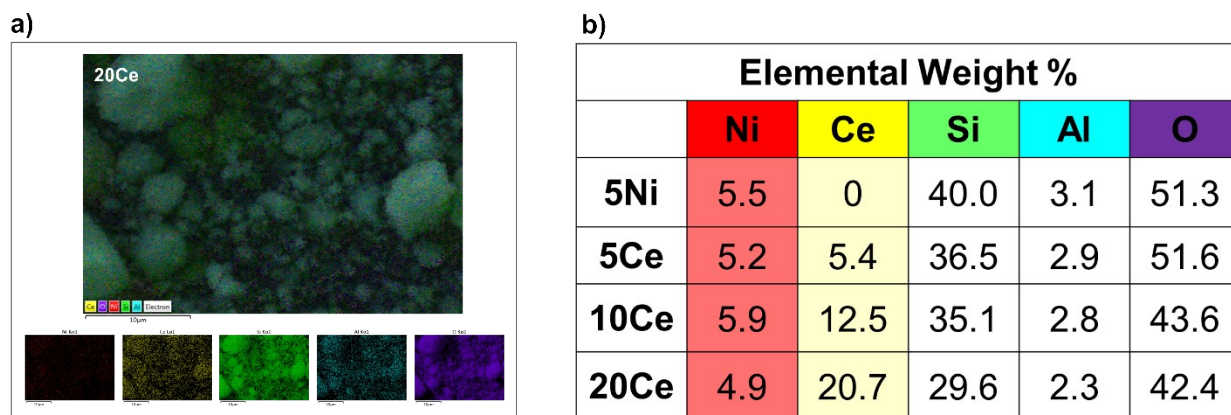


Figure S4. a) SEM-EDX elemental mapping of 5Ni20Ce/BEA (20Ce) catalyst and b) elemental composition for 5Ni/BEA (5Ni) and Ce-promoted 5Ni/BEA catalysts (%Ce = 5, 10, 20).

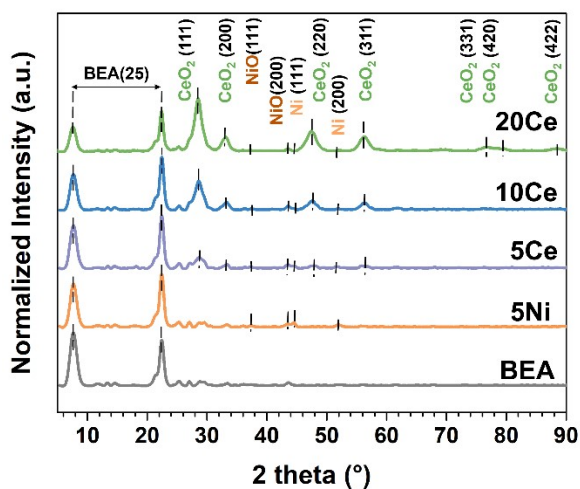


Figure S5. XRD patterns for BEA(25), 5Ni/BEA (5Ni), and Ce-promoted 5Ni/BEA (%Ce = 5, 10, 20) catalysts.

Diffraction peaks for Ni/NiO are barely detected in 20Ce catalysts due to small particle size (TEM $d_{\text{avg}} \sim 3.6 \pm 1.2$ nm).

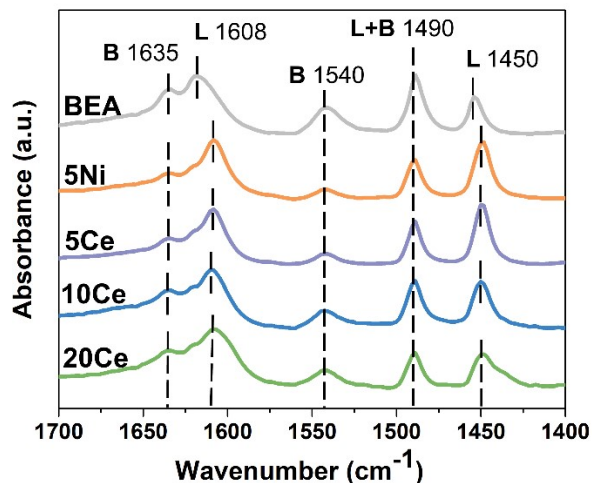


Figure S6. FTIR spectra of pyridine adsorption collected at 300 °C under Ar flow for BEA(25), 5Ni/BEA (5Ni), and Ce-promoted 5Ni/BEA catalysts (%Ce= 5, 10, 20).

Integration of Brønsted and Lewis acid sites at peak positions of 1540 and 1450 cm^{-1} and molar extinction coefficients¹ used to calculate acid site densities. Brønsted acid sites denoted by “B” and Lewis acid sites denoted by “L”.

Table S3. Assigned peak position (BE) and relative area (%) for $\text{Ni}2p_{3/2}$ XPS spectra of Ce-promoted 5Ni/BEA catalysts (%Ce= 0, 5, 10, 20).

Catalyst	Ni^0 BE (eV)	NiO BE (eV)	Ni(OH)_2 BE (eV)	Ni^0 %	NiO %	Ni(OH)_2 %
5Ni	852.6	853.6	856.9	0.3	61.8	38.0
5Ce	852.8	853.6	856.6	2.7	48.8	48.5
10Ce	852.6	853.8	856.6	7.2	43.2	49.6
20Ce	852.7	853.9	856.1	12.5	29.3	58.2

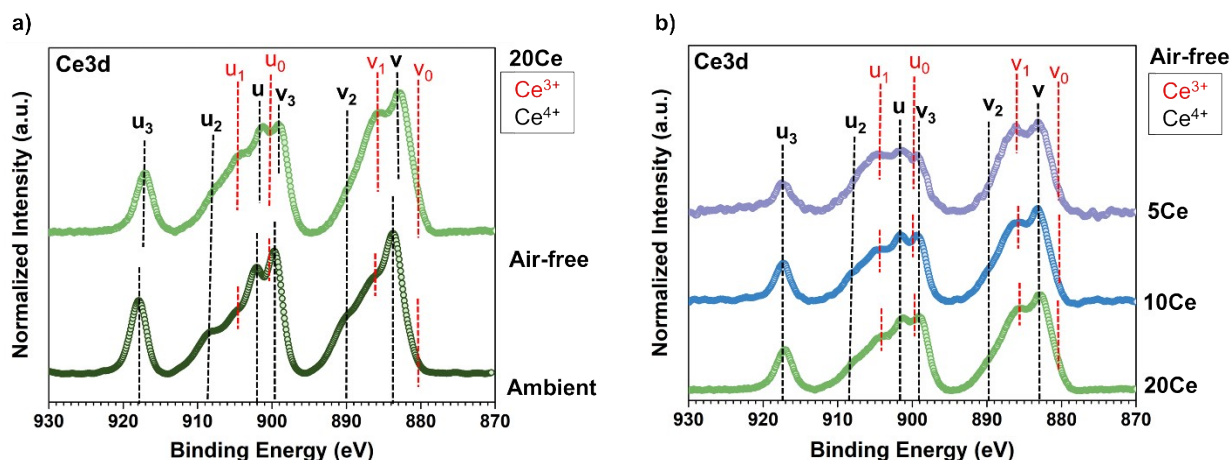


Figure S7. a) Comparison of 5Ni20Ce/BEA (20Ce) XPS spectra under air-free and ambient conditions. b) Air-free XPS spectra of Ce3d region for Ce-promoted 5Ni/BEA (%Ce= 5, 10, 20) catalysts. XPS spectra normalized to C1s at 284.8 eV.

XPS was performed on the Ce-promoted 5Ni/BEA (%Ce= 5, 10, 20) catalysts to verify Ni and Ce's co-reduction through the presence of Ce^{3+} species (degree of ceria reduction). In Figure S7a, XPS measurements for fresh 20Ce catalyst were conducted in two different conditions: air free and ambient. For air-free XPS, the catalyst was pre-reduced at 350 °C for 2 h in 50:50 H_2/He flow in a quartz tube, which was then sealed at both ends (via valves) and transferred into an N_2 glove box for sample preparation. A vacuum transfer vessel was used to transport the sample holder from the glove box to the instrument for measurements without air exposure. For ambient XPS, the catalysts were pre-reduced at the same conditions but were prepared directly on the benchtop and exposed to air during the process. The Ce3d spectra contain peaks that correlate to the spin-orbital doublets of 3d3/2 and 3d5/2, denoted by “u” and “v,” respectively. Spectra of pure CeO_2 exhibit 6 peaks with only 1 chemical state (Ce^{4+}) but partially reduced CeO_2 includes 4 additional final spin-orbital state contributions from Ce^{3+} species.²⁻⁴ Based on literature nomenclature, these 10 peaks can be represented as v, v₂, v₃, u, u₂, u₃ which is associated with Ce^{4+} (denoted in black) and v₀, v₁, u₀, u₁ for Ce^{3+} (denoted in red).²⁻⁴

TPR (Figure 3a) analysis demonstrated the reduction of pure CeO_2 occurs at temperatures above 450 °C. As the Ce loading was increased, the co-reduction of both Ni and Ce at lower temperatures (< 350 °C) was observed. Ambient XPS measurement (Figure S7a) of the exposed 20Ce catalyst exhibits prominent v, v₂, v₃, u, u₂, and u₃ peaks, indicating that CeO_2 exists primarily in a Ce^{4+} state due to its highly oxophilic nature. However, under an air-free atmosphere (Figure S7a), we observe the growth of peaks u₁ (~904 eV) and v₁ (~886 eV), as well as the broadening of peaks u₂ (~908 eV), v₃ (~917 eV), and v₂ (~889 eV), indicating the formation of Ce^{3+} species.^{5, 6} Furthermore, Figure S7b shows that the Ce-promoted catalysts all exhibit peaks associated with the Ce^{3+} electronic state, providing additional evidence for the partial reduction of CeO_2 and formation of oxygen vacancies under reaction conditions (300 °C, 30 bar H_2).

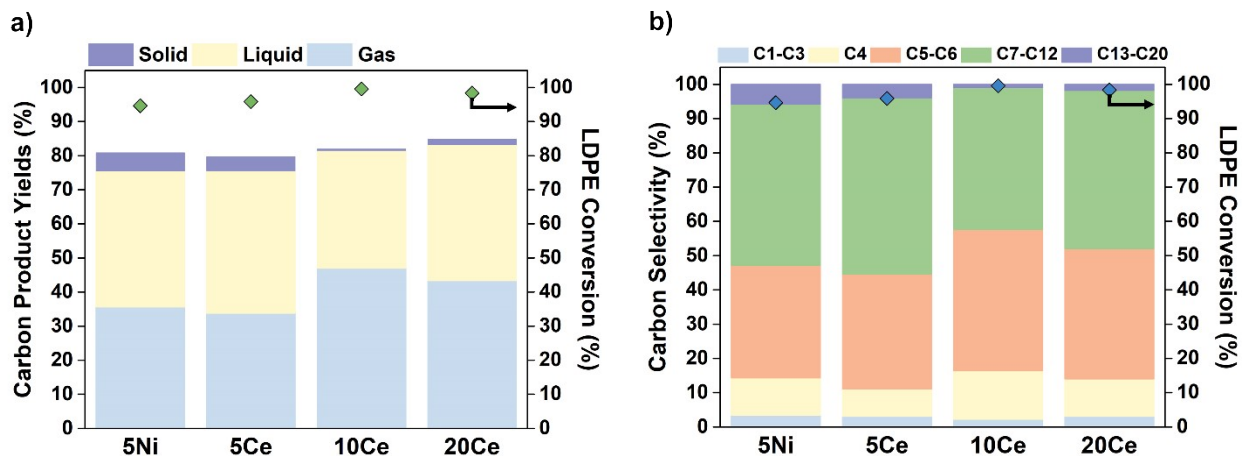


Figure S8. Full conversion experiments conducted for TGA analysis of spent catalyst for coking analysis. **a)** Hydrocracking mass yield of carbon products (solid, liquid/oil, and gas) and conversion for 2 g LDPE using 0.025 g 5Ni%Ce/BEA (% = 0, 5, 10, 20) at 300 °C, 30 bar H₂, for 3.5 h. **b)** LDPE hydrocracking product selectivity distributions.

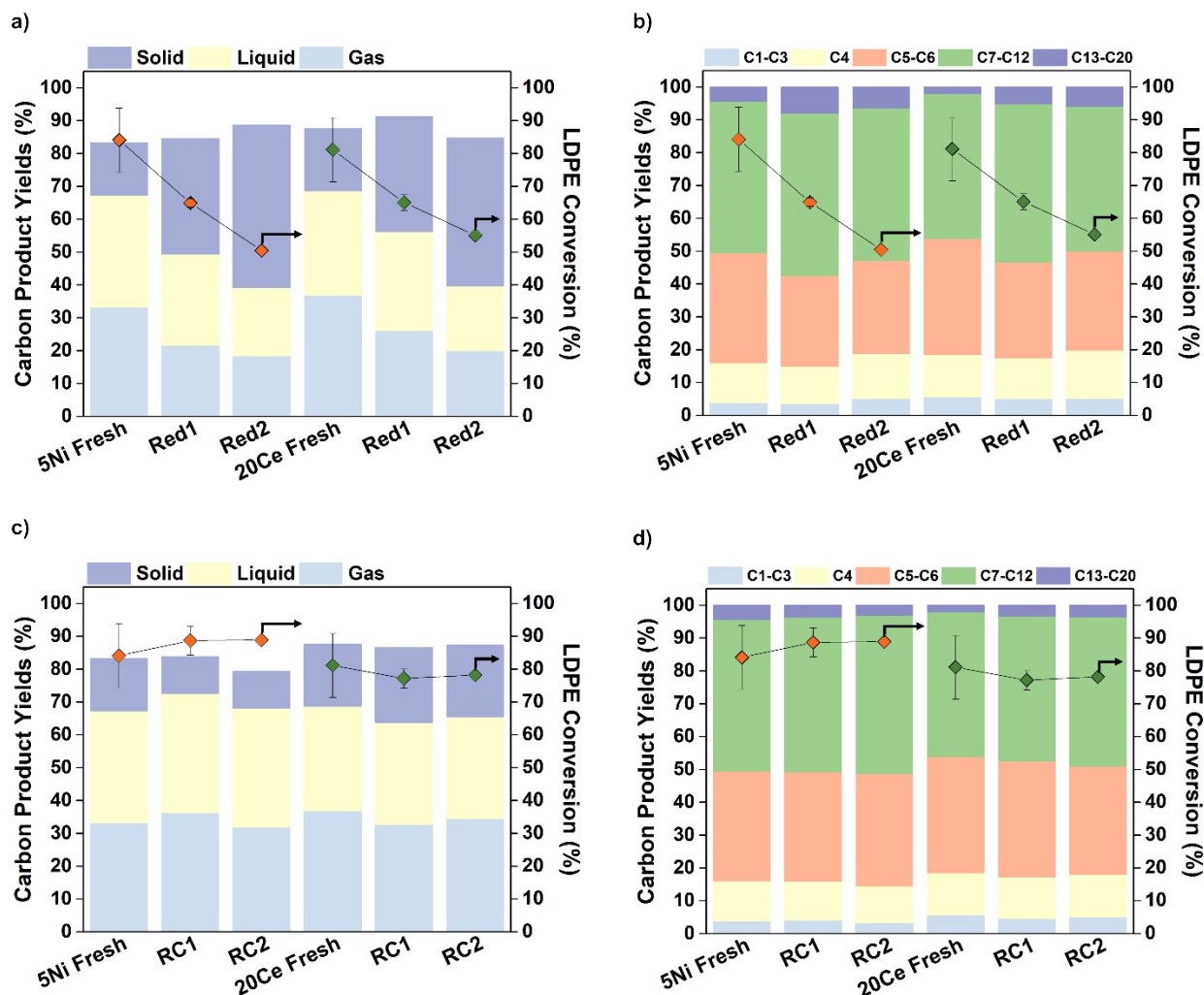


Figure S9. Catalyst reusability tests for Ni/BEA (5Ni) and 5Ni20Ce/BEA (20Ce) catalysts after 3 reaction cycles. **a)** Hydrocracking activity and **b)** selectivity of non-regenerated (reduction only; red) spent catalysts. **c)** Hydrocracking activity and **d)** selectivity of regenerated (calcination and reduction; RC) spent catalysts. Reaction conditions: 2 g LDPE, 0.05 g of catalyst, 300 °C, 30 bar H₂. Error bars for the fresh catalyst represent the standard deviation for 6 repeated experiments. For spent catalysts used in cycle 1 of the reuse, the error bars represent the standard deviation for duplicate experiments.

Spent catalysts were combined from 6 reactions starting from fresh catalysts. To compare the fresh catalysts at similar conversions, the reaction time for 20Ce catalyst was reduced to 45 min vs. a 1 h reaction time for the 5Ni catalysts. Spent catalysts were extracted from the residual reaction solid through dissolution in hot toluene, filtered, and then vacuum-dried overnight. Spent catalysts without regeneration for reuse cycles 1 and 2 (denoted as Red1 and Red2) were reduced under a 50:50 H₂/He flow (mL/min) at 350 °C for 2 h prior to reuse. Regenerated spent catalysts for cycles 1 and 2 (denoted as RC1 and RC2) were first calcined at 550 °C for 4 h and then reduced at 350 °C for 2 h in 50:50 H₂/He flow (mL/min) prior to reuse.

Direct reuse of the catalyst without regeneration resulted in a significant loss of hydrocracking activity (Figure S9a) for 5Ni and 20Ce catalysts. Compared to the fresh catalysts,

a 41% and 35% reduction in LDPE conversion was observed after 2 reuses over the 5Ni and 20Ce catalysts, respectively. The overall product distributions did not change significantly (Figure S9b), except for a slight increase in selectivity toward heavier (C_{13} - C_{20}) products due to the lower cracking rates. After the first reuse, both catalysts exhibited deactivation due to heavy coke species that remain adsorbed at temperatures above 350 °C (Figure S10a&b), which were not observed on the fresh catalysts (Figure S11). After 2 reuse cycles, the 20Ce still exhibited slightly higher activity (Figure S9a) and stronger resistance to coking (8.2%) compared to the 5Ni catalyst (12.7%), as shown in Figure S10a&b. CeO_2 promotes the hydrogenation of adsorbed species on the Ni, thereby suppressing the formation of coke deposits. However, the Brønsted acid sites responsible for cracking likely experience significant coking after continued reuse, resulting in a dramatic loss in activity. Furthermore, heavy coke may also oligomerize and migrate during reduction, contributing to additional blocking of pores and physical coverage of Ni, BAS, and CeO_2 as well.

The spent 5Ni and 20Ce catalysts were fully regenerable (*via* calcination and reduction). Both regenerated spent catalysts maintained comparable activity and naphtha selectivity to the fresh catalysts after 2 reuse cycles (Figure S9c&d). Regeneration through calcination was shown to remove all the coke (Figure S10c&d) responsible for catalyst deactivation and is comparable to the fresh catalysts (Figure S11). Some residual light impurities (< 350 °C) remained, but these species can easily be removed under reaction conditions. These results demonstrate that 5Ni and 20Ce-promoted catalysts are reusable, and regeneration can fully recover their performance.

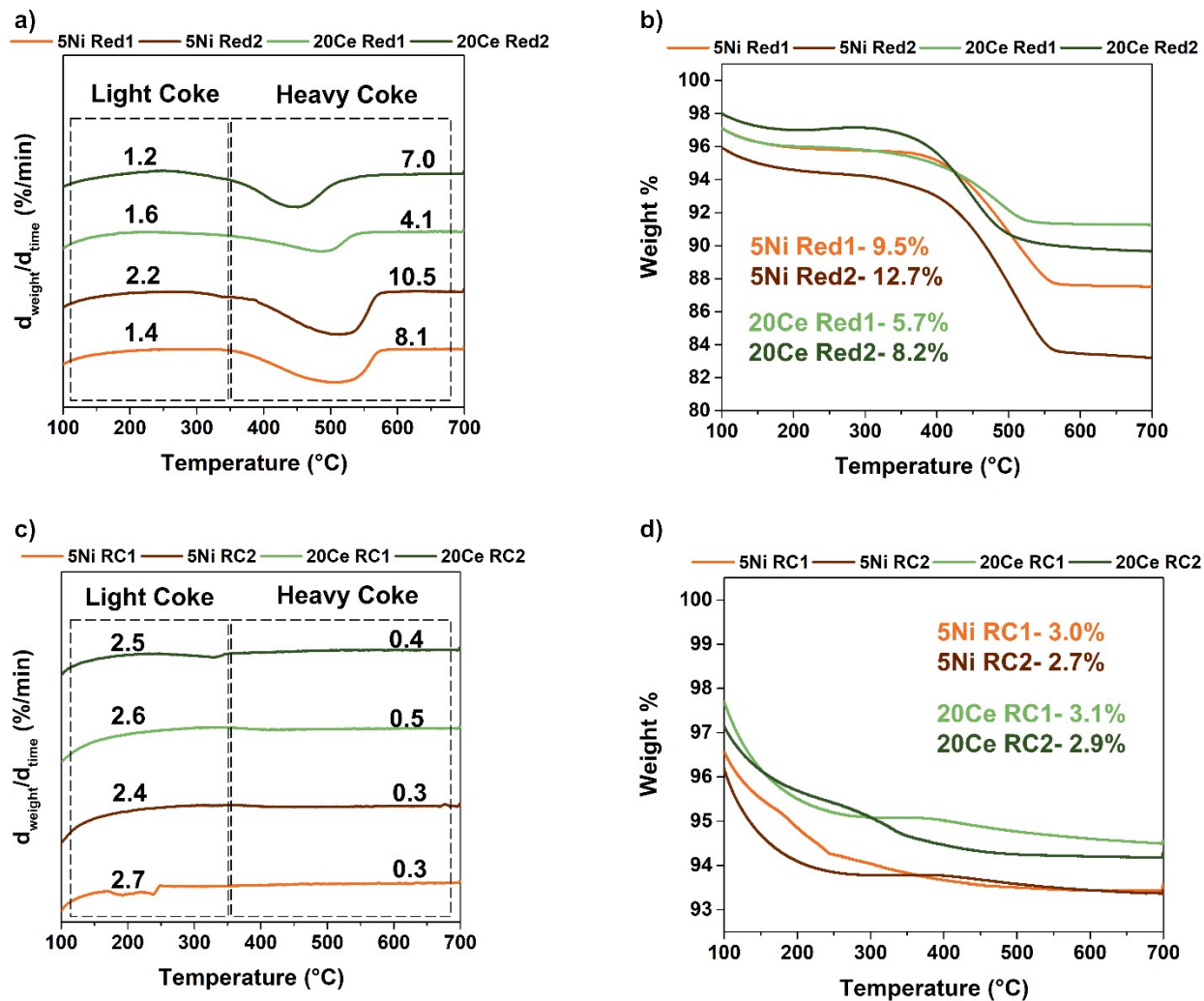


Figure S10. a) TGA derivative weight loss (%/min) and b) total weight % loss thermograms of spent 5Ni/BEA (5Ni) and 5Ni20Ce/BEA (20Ce) catalyst in air atmosphere after reuse cycles 1 and 2 without regeneration, reduction only (denoted as Red1 and Red2). c) TGA derivative weight loss and d) total weight % loss thermograms of regenerated (calcination and reduction) spent catalyst after reuse cycles 1 and 2 (denoted as RC1 and RC2).

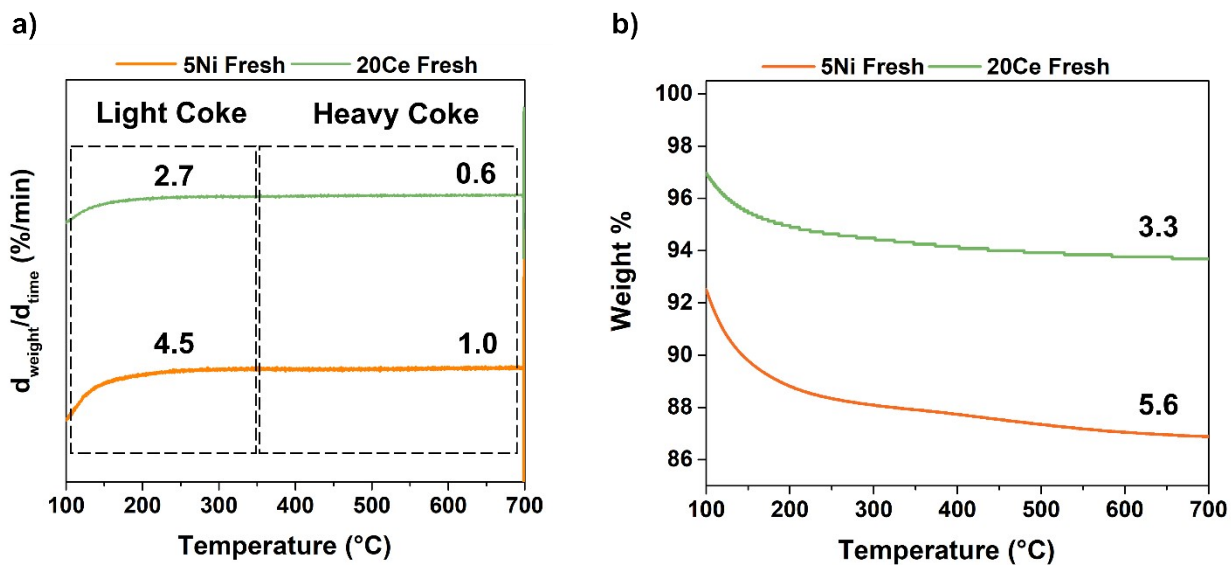


Figure S11. a) TGA derivative weight loss (%/min) and b) total weight % loss thermograms of fresh 5Ni/BEA (5Ni) and 5Ni20Ce/BEA (20Ce) catalyst in air.

Fresh catalysts do not exhibit any coking. The weight loss measured of the fresh 5Ni catalyst is greater than that of the regenerated reused 5Ni catalyst (Figure S10c&d), likely due to water presence. Fresh catalysts were stored at ambient conditions on the benchtop prior to measurements. Regenerated catalysts were dried in a vacuum oven overnight prior to measurements, reducing the moisture on the sample.

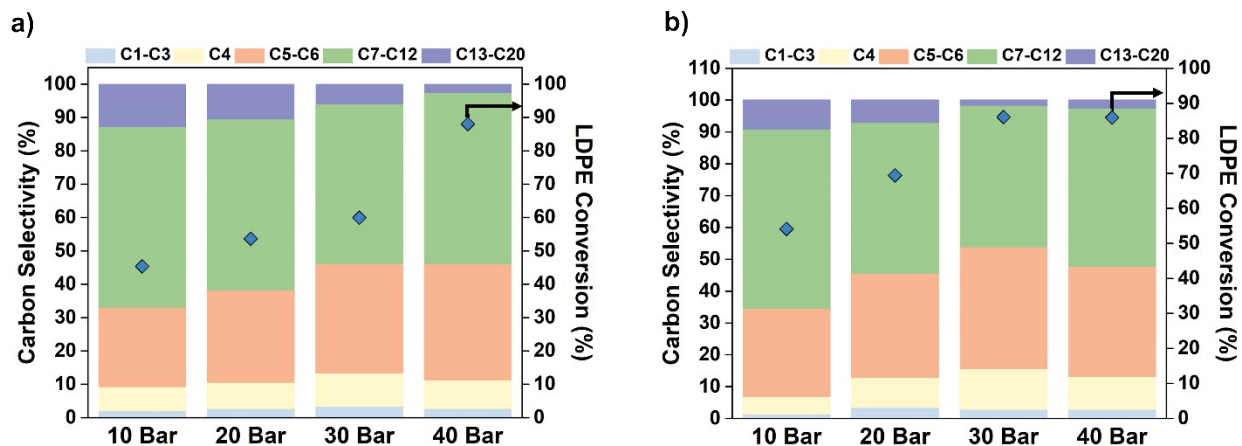


Figure S12. LDPE hydrocracking selectivity and conversion at varying H_2 pressures for a) 5Ni/BEA (5Ni) and b) 5Ni20Ce/BEA (20Ce) catalysts. Reaction conditions: 2 g LDPE, 0.025 g catalyst, 300 °C, 1 h.

As the H_2 pressure decreases, heavier products are favored (C_{13} - C_{20}) due to the lowered rates of hydrocracking.

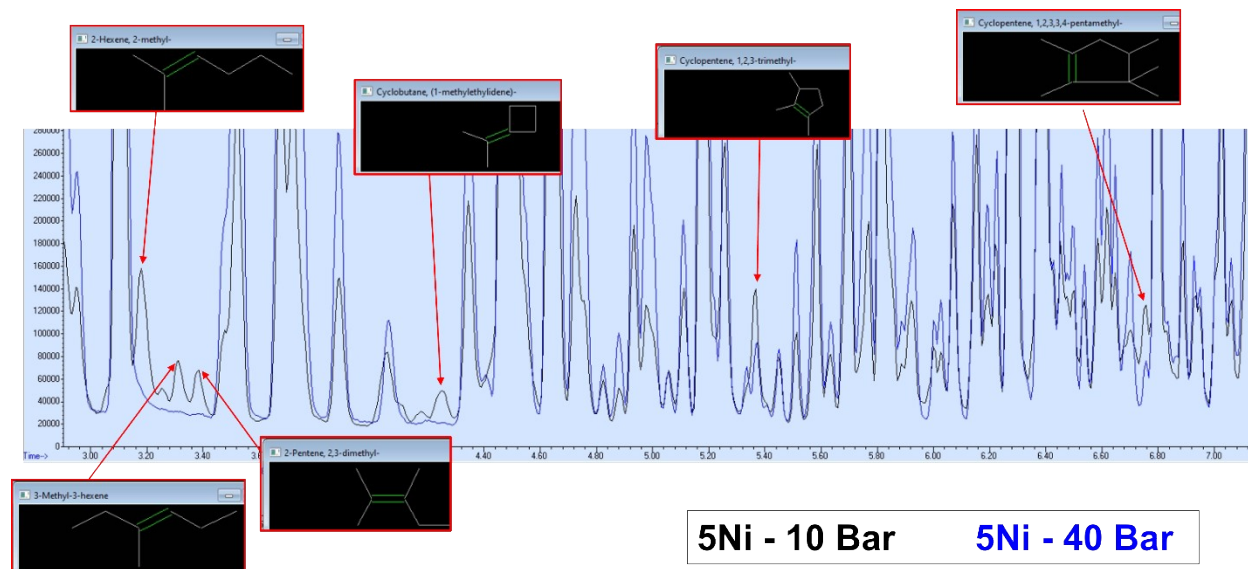


Figure S13. GC-MS chromatogram depicting olefin intermediates and cyclic alkanes in liquid products from LDPE hydrocracking at P_{H_2} =10 bar over 5Ni/BEA (5Ni). Reaction conditions: 2 g LDPE, 0.025 g catalyst, 300 °C, 1 h.

Table S4. H₂ consumption for 5Ni/BEA (5Ni) and 5Ni20Ce/BEA (20Ce) measured by H₂ pulse chemisorption using 10 consecutive pulses.

Catalyst	H ₂ consumed (μmol/g _{cat})
5Ni	2.99
20Ce	5.14

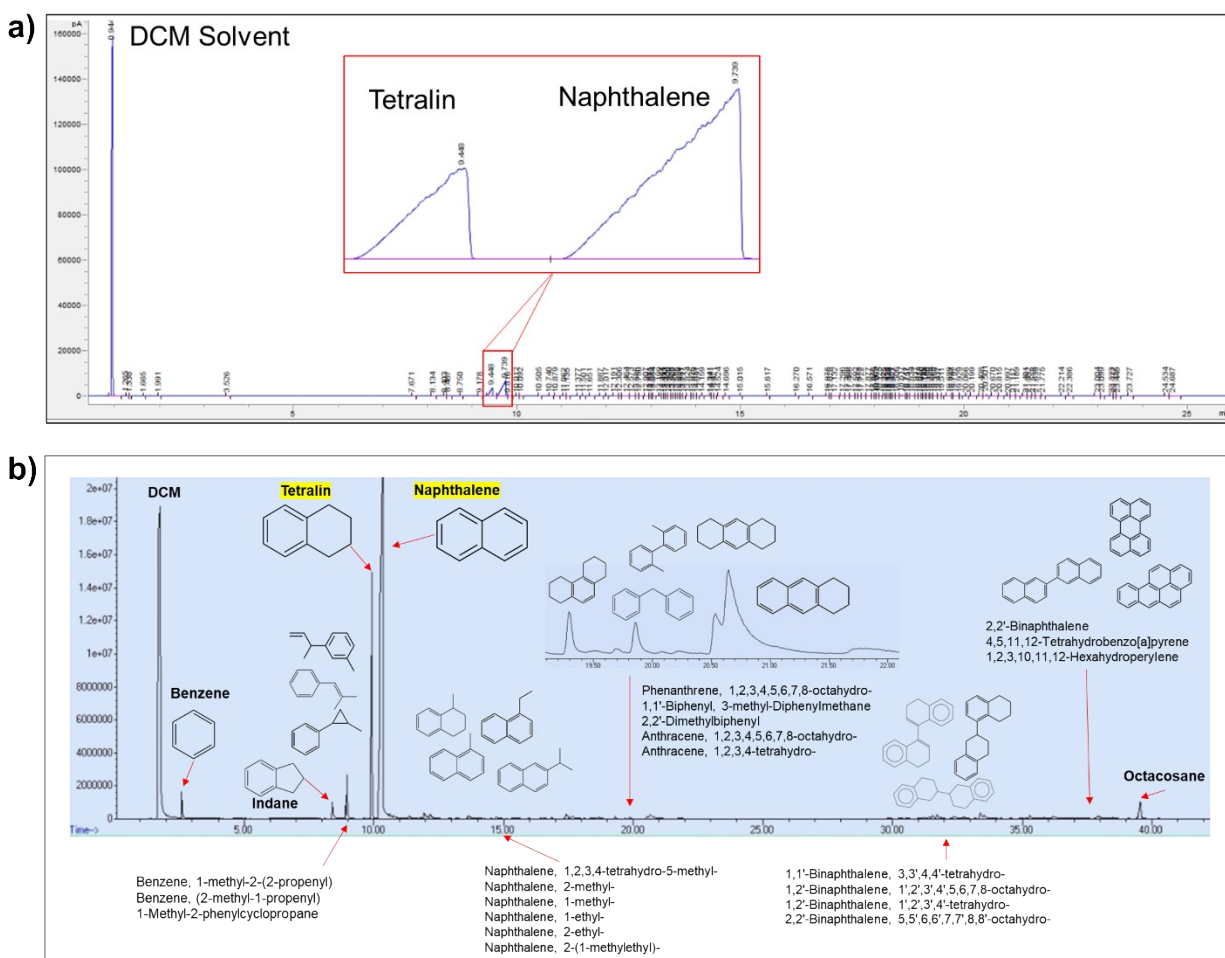


Figure S14. a) Typical GC chromatogram and b) GC-MS chromatogram for the liquid products obtained from the hydrogenation of naphthalene over 5Ni20Ce/BEA (20Ce) catalyst. Reaction conditions: 1 g naphthalene, 0.025 g catalyst, 300 °C, 1 h.

Hydrogenation reaction conditions were chosen to mimic hydrocracking experiments and limit naphthalene conversion to target direct hydrogenation to tetralin (the major product).^{7, 8} Only naphthalene and tetralin yields were quantified (based on calibration, Figure S15) to calculate naphthalene conversion and tetralin selectivity. As hydrogenation was maintained at conversions

of ~35% (Figure 5b), contributions of aromatic and polyaromatic products arising from side reactions, including cracking, isomerization, ring opening, condensation, and dealkylation, were not significant and were disregarded in the analysis.

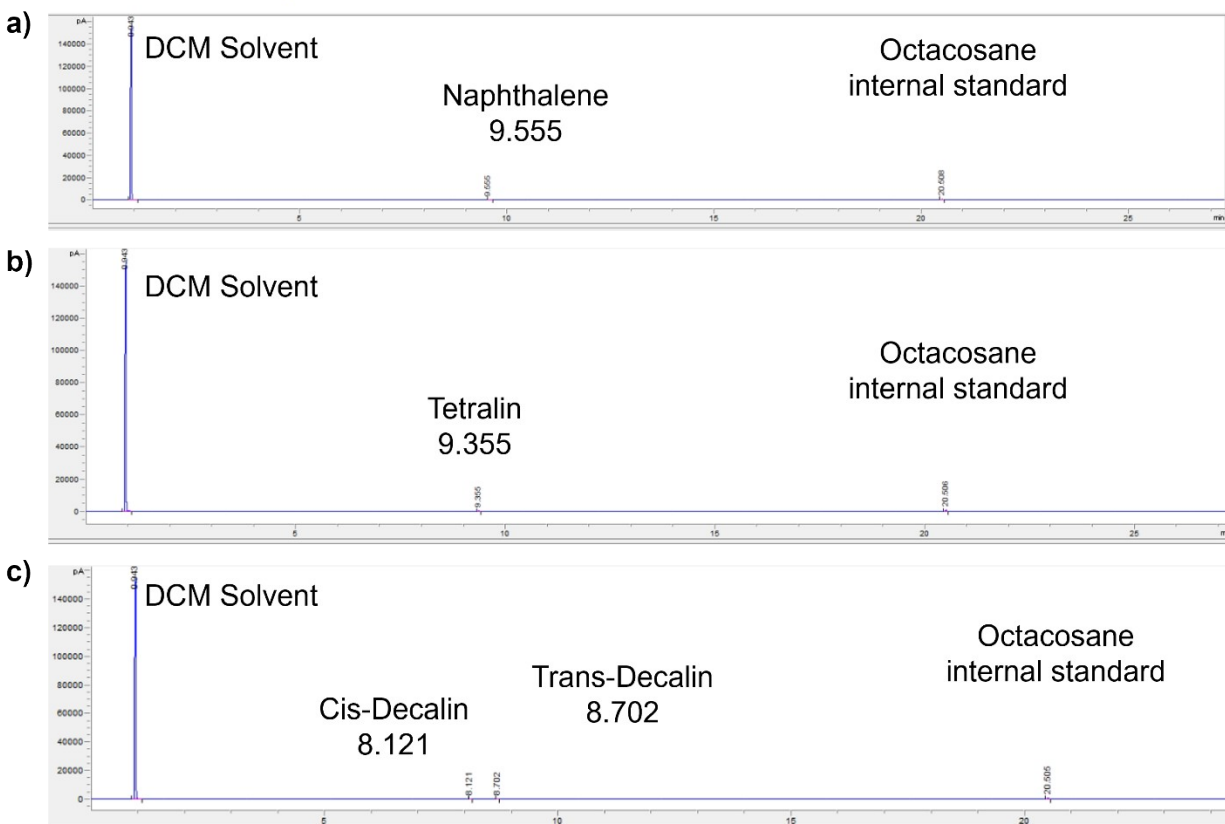


Figure S15. GC chromatogram of the naphthalene, tetralin, and decalin calibration standards for the hydrogenation probe reactions.

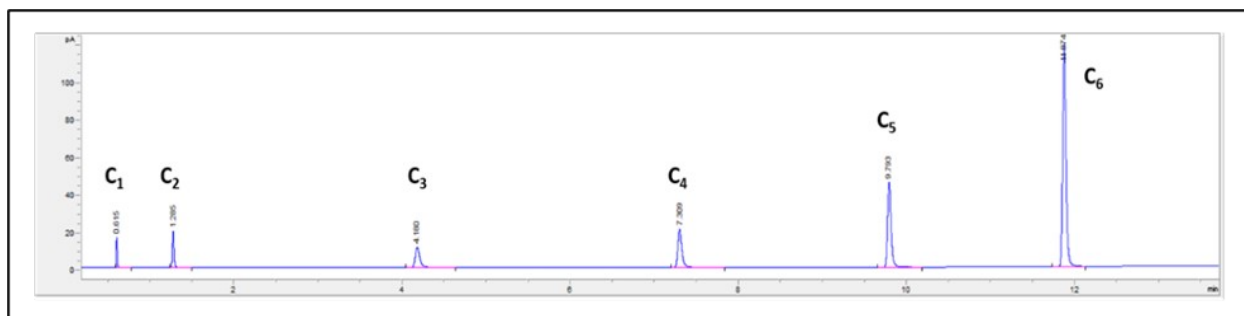


Figure S16. GC chromatogram of the gas hydrocarbon-mix calibration standard for hydrocracking reactions.

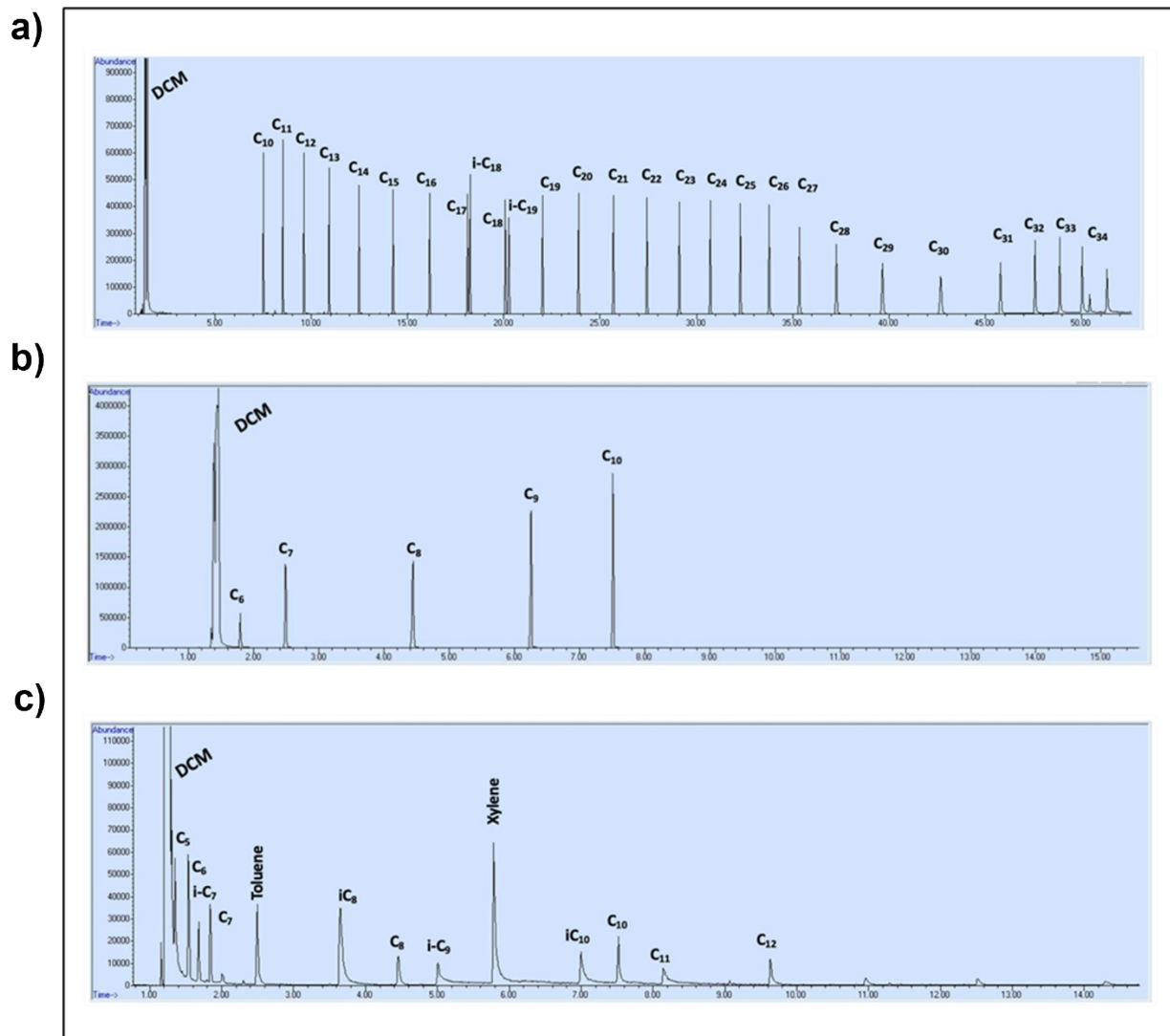


Figure S17. GC-MS chromatogram of the liquid hydrocarbon-mix. **a)** Calibration standard 1, **b)** calibration standard 2, and **c)** calibration standard 3 for hydrocracking reactions.

References

1. M. Tamura, K.-i. Shimizu and A. Satsuma, *Applied Catalysis A: General*, 2012, **433**, 135-145.
2. A. Pfau and K. Schierbaum, *Surface Science*, 1994, **321**, 71-80.
3. D. J. Morgan, *Surface and Interface Analysis*, 2023, **55**, 845-850.
4. E. Bêche, P. Charvin, D. Perarnau, S. Abanades and G. Flamant, *Surface and Interface Analysis: An International Journal devoted to the development and application of techniques for the analysis of surfaces, interfaces and thin films*, 2008, **40**, 264-267.
5. M. Romeo, K. Bak, J. El Fallah, F. Le Normand and L. Hilaire, *Surface and Interface Analysis*, 1993, **20**, 508-512.
6. S. Soni, V. Vats, S. Kumar, B. Dalela, M. Mishra, R. Meena, G. Gupta, P. Alvi and S. Dalela, *Journal of Materials Science: Materials in Electronics*, 2018, **29**, 10141-10153.
7. Q. Wang, H. Fan, S. Wu, Z. Zhang, P. Zhang and B. Han, *Green Chemistry*, 2012, **14**, 1152-1158.
8. P. A. Rautanen, M. S. Lylykangas, J. R. Aittamaa and A. O. I. Krause, *Industrial & engineering chemistry research*, 2002, **41**, 5966-5975.